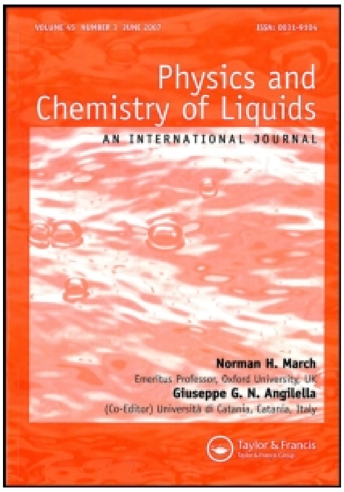

Physics and Chemistry of Liquids
Publication details, including instructions for authors and subscription information:
http://www.informaworld.com/smpp/title~content=t713646857

# High temperature and high pressure volumetric properties of (methanol + [BMIM$^+$][OcSO$_4^-$]) mixtures

I. M. Abdulagatov[a]; J. Safarov[bc]; T. Guliyev[c]; A. Shahverdiyev[c]; E. Hassel[b]
[a] Geothermal Research Institute of the Dagestan Scientific Center of the Russian Academy of Sciences, Makhachkala, Dagestan, Russia [b] Lehrstuhl für Technische Thermodynamik, Universität Rostock, Rostock, Germany [c] Heat and Refrigeration Techniques, Azerbaijan Technical University, Baku, Azerbaijan

**To cite this Article** Abdulagatov, I. M. , Safarov, J. , Guliyev, T. , Shahverdiyev, A. and Hassel, E.(2009) 'High temperature and high pressure volumetric properties of (methanol + [BMIM$^+$][OcSO$_4^-$]) mixtures', Physics and Chemistry of Liquids, 47: 1, 9 — 34

**To link to this Article: DOI:** 10.1080/00319100802372106

**URL:** http://dx.doi.org/10.1080/00319100802372106

*Physics and Chemistry of Liquids*
Vol. 47, No. 1, February 2009, 9–34

Taylor & Francis
Taylor & Francis Group

# High temperature and high pressure volumetric properties of (methanol + $[BMIM^+][OcSO_4^-]$) mixtures

I.M. Abdulagatov[a*†], J. Safarov[bc], T. Guliyev[c],
A. Shahverdiyev[c] and E. Hassel[b]

[a]*Geothermal Research Institute of the Dagestan Scientific Center of the Russian Academy of Sciences, Makhachkala, Dagestan, Russia;* [b]*Lehrstuhl für Technische Thermodynamik, Universität Rostock, Rostock, Germany;* [c]*Heat and Refrigeration Techniques, Azerbaijan Technical University, Baku, Azerbaijan*

(*Received 30 May 2008; final version received 28 July 2008*)

The $(p, \rho, T)$ and some derived volumetric properties such as excess, partial and apparent molar volumes of $[BMIM^+][OcSO_4^-]$ in methanol at temperatures $T = (298.15–398.15)$ K and pressures up to $p = 40$ MPa have been measured with a vibrating-tube densimeter. Measurements were made at seven concentrations of $x = (0.0388, 0.1351, 0.2785, 0.4961, 0.7497, 0.9312$ and $1.0)$ mole fraction of $[BMIM^+][OcSO_4^-]$. The total uncertainty of density, temperature, pressure and concentration measurements were estimated to be less than $0.15\,kg\,m^{-3}$, 15 mK, 5 kPa and $10^{-4}$ mole fraction, respectively. The uncertainties reported in this article are expanded uncertainties at the 95% confidence level with a coverage factor of $k = 2$. The effect of temperature, pressure and concentration on the density and derived volumetric properties was studied. The measured densities were used to develop a Tait-type equation of state (EOS) for the mixture and the pure components. The derived values of apparent molar volumes were extrapolated to zero concentration using Pitzer's ion-interaction model to calculate the values of apparent molar volumes (or partial molar volumes) at infinite dilution. The method of correlation function integrals is used to study the structural and thermodynamic properties of dilute methanol + ILs mixtures. The structural properties, such as direct and total correlation function integrals and cluster size (coordination number), were calculated using the Krichevskii function concept and EOS for the mixture at infinite dilution.

**Keywords:** 1-butyl-3-methylimidazolium octylsulphate; apparent molar volume; correlation function integrals; density; equation of state; excess molar volume; ionic liquid; methanol; partial molar volume

## 1. Introduction

The ionic liquids (ILs) have potential uses for new chemical processes and technologies (fuel cell, separations, industrial cleaning, lubricants, new high energy density materials as fuels and monopropellants, heat transfer fluid, reaction media for synthesis, catalysis and biocatalysis) [1–5]. ILs are of interest due to their unique thermodynamic properties – low

---

*Corresponding author. Email: ilmutdin@boulder.nist.gov

†Current address: Physical and Chemical Properties Division, National Institute of Standards and Technology, 325 Broadway, Boulder, Colorado 80305, USA.

ISSN 0031–9104 print/ISSN 1029–0451 online

DOI: 10.1080/00319100802372106
http://www.informaworld.com

vapour-pressure – which can be custom synthesised, water-miscible or water-immiscible, nonvolatile, noninflammable, excellent solvating capability, thermally stable, recyclable, large liquid gap (about 200°C between melting and decomposition temperature). Due to nearly negligible vapour pressure ILs do not generate noxious volatile residues. Due to their unique properties, ILs have also been suggested as green replacements for traditional volatile toxic organic solvents, supercritical fluid, and for organic solvents in multiphase bioprocess operations [6]. Most ILs have a high viscosity and relative low conductivity. The thermodynamic and transport properties depend on their large cation (alkylimidazolium, alkylpyridinium, alkylphosphonium, quarternary ammonium) and on their inorganic anion having a delocalised charge ($PF_6^-, BF_4^-$ and $(Tf_2)N$). Therefore, ILs of various thermodynamic properties can be synthesised by changing the cation or the anion (charge distribution on the ions). Any technological processes involving ILs require accurate knowledge of their thermodynamic properties. Their H-bonding ability, polarity, and the dispersive interactions are also the factors that influence thermodynamic and transport properties. There is much data reported on the thermophysical [7] and structural [8] properties for ILs. However, there is still no deep understanding of the effect of microstructure and chemical constituents on their thermodynamic properties. Very little is known about how thermodynamic properties of ILs relate to structure and constituents. New accurate experimental thermodynamic data are required for the development of accurate predictive theoretical models. Basically, our knowledge of the properties of ILs is somewhat empirical. A detailed understanding of the thermodynamic properties of ILs on the microscopic (molecular) level follows, to extend and amplify the possibility of technological applications.

A literature survey revealed that only one experimental dataset, reported by Domańska *et al.* [9], is available for the density of methanol + [BMIM$^+$][OcSO$_4^-$] solutions. These measurements were performed at 298.15 K and at 0.1 MPa only in the whole concentration range using an Anton Paar DMA 602 VTD. No density data are available for this mixture under pressure and high temperatures. Very few (only four datasets) measurements are available in the literature at high temperatures and high pressures for pure [BMIM$^+$][OcSO$_4^-$] (Table 1). In Table 1, a summary of all the available density measurements, to our knowledge, is presented for pure [BMIM$^+$][OcSO$_4^-$]. Machida *et al.* [10] and Dávila *et al.* [11] reported densities of pure [BMIM$^+$][OcSO$_4^-$] at high temperatures and at high pressures, while the measurements by Domańska *et al.* [9] and Wandschneider [12] were performed at atmospheric pressure and in a temperature range from 278 to 328 K. Most measurements were made with VTD with

Table 1. Summary of the density measurements for pure [BMIM$^+$][ OcSO$_4^-$ ].

| First author | Purity | Year | Method | Property | Temperature, $T$ ($K$) | Pressure, $p$ (MPa) | Uncertainty |
|---|---|---|---|---|---|---|---|
| Machida [10] | > 95 wt.% | 2008 | PC[a] | $p, \rho, T$ | 313–473 | 200 | 0.06% |
| Domańska [9] | 98 wt.% | 2006 | VTD[a] | $\rho, T$ | 298 | 0.1 | NA[a] |
| Dávila [11] | > 95 wt.% | 2007 | VTD[a] | $p, \rho, T$ | 318–428 | 60 | $10^{-4}$ g cm$^{-3}$ |
| Wandschneider [12] | 0.18 wt% ($H_2O$ content) | 2008 | VTD[a] | $\rho, T$ | 278–328 | 0.1 | $10^{-4}$ g cm$^{-3}$ |

Note: [a]PC – pycnometer; VTD – vibrating tube densimeter; NA – not available.

uncertainty within 0.01–0.06% depending on temperature and pressure. Recent measurements by Machida *et al.* [10] were performed with a pycnometer at ambient pressures and a bellows type apparatus at elevated pressures. They also developed a Tait-type EOS for pure ILs.

The main objective of the work is to provide new accurate experimental density data for methanol + [BMIM$^+$][OcSO$_4^-$] mixtures and pure [BMIM$^+$][OcSO$_4^-$] at high temperatures (up to 398.15 K) and at high pressures (up to 40 MPa) for the entire concentration range using a VTD technique, which have been previously used for accurate measurements on other ILs containing mixtures (Abdulagatov *et al.* [13–17]). In the present work the temperature and pressure ranges were considerably expanded in which density data for the mixture are available. The Tait type equation of state (EOS) for methanol + [BMIM$^+$][OcSO$_4^-$] mixture and pure components were also developed, which accurately reproduce the present density results. The measured and derived volumetric properties (density, excess, apparent, and partial molar volumes) data methanol + ([BMIM$^+$][OcSO$_4^-$] were interpreted in terms of structural properties (direct and total correlation function integrals, coordination number).

## 2. Experimental

The $(p, \rho, T)$ properties of methanol + [BMIM$^+$][OcSO$_4^-$] solutions and pure [BMIM$^+$][OcSO$_4^-$] were studied using a high pressure – high temperature vibrating tube densimeter DMA HPM. The method (apparatus, procedure of measurements, calibration procedure, and uncertainty assessment) has been described fully in our previous publications [13–17]. Only essential information will be given here. The vibration tube (length 15 cm, U radius of 1 cm, OD 6 mm, ID 2 mm, volume of the liquid in the tube was 2 cm$^3$) was made with corrosion resistance and a good fabric material (Hastelloy C-276, nickel–molybdenum–chromium–tungsten alloy). For the pressure measurement, a pressure transducer (model P-10, WIKA, Switzerland) was used. For this method the density of a fluid under study $\rho$ can be expressed explicitly as a linear function of the square of the period of vibrating $\tau$

$$\rho = A - B\tau^2, \tag{1}$$

or

$$\rho - \rho_0 = B\left(\tau^2 - \tau_0^2\right), \tag{2}$$

where $A$ and $B$ are the calibrating constants as a function of temperature and pressure; subscript 0 relates to the reference fluid. The parameters $A$ and $B$ can be determined for each temperature and pressure using minimum two reference fluids (see our previous publications [13–17]). The uncertainty in the pressure measurements is 5 kPa. The temperature was measured using a (ITS-90) Pt100 thermometer with an uncertainty of 15 mK. The uncertainty in density measurements is 0.01 kg m$^{-3}$ at low pressures (near atmospheric pressure) and 0.15 kg m$^{-3}$ at high pressures (the combined expanded uncertainty, coverage factor is $k = 2$). This leads to maximum relative uncertainties of 0.02% for the performed measurements at high temperatures and high pressures. To check the apparatus and procedures of the measurements, and the accuracy of calibration before engaging in measurements on solution, the density of triple-distilled water and a reference fluid (methanol) was measured and compared with the values calculated from IAPWS [18] and IUPAC [19] formulations. Excellent agreement within 0.003% at atmospheric pressure and 0.04% at high pressures and high temperatures were observed between the measured densities for pure methanol using the same apparatus in our previous work [20] and the values calculated with reference fundamental IUPAC [19] EOS.

$[\mathrm{BMIM}^+][\mathrm{OcSO}_4^-]$ (stated purity >98 mass%) was supplied from Solvent Innovation, Germany. Methanol was supplied from Merck (Germany) with a purity of 99.9 mass% and used without further purification. The water content in the ILs ($[\mathrm{BMIM}^+][\mathrm{OcSO}_4^-]$) before dehydration was <1000 ppm. To reduce the water content and volatile compounds to negligible values, the sample was thoroughly dried before use under a reduced pressure of about 0.5 Pa by heating at $T = 373.15$ K for 48 h. The sample is kept as dry as possible (no contact with air). After this procedure, the water content in the $[\mathrm{BMIM}^+][\mathrm{OcSO}_4^-]$ was determined with a coulometric 'Aquapal' Karl Fischer. The final water content in our ILs sample was quite low (162 ± 10 ppm). The solutions were prepared by mass using an electronic scale with a resolution of $10^{-4}$ g.

## 3. Results and discussion

### 3.1. *Density*

Measurements of the densities of methanol + $[\mathrm{BMIM}^+][\mathrm{OcSO}_4^-]$ solutions at seven concentrations of $x = (0.0388, 0.1351, 0.2785, 0.4961, 0.7497, 0.9312$ and $1.0)$ mole fraction of $[\mathrm{BMIM}^+][\mathrm{OcSO}_4^-]$ were carried out at temperatures between 298.15 and 398.15 K and at pressures up to 40 MPa. Table 2 presents the experimental temperature, density, pressure and concentration values for methanol + $[\mathrm{BMIM}^+][\mathrm{OcSO}_4^-]$ solutions. The measured results are also shown in Figures 1–3 in $\rho$-$p$, $\rho$-$T$ and $\rho$-$x$ planes for the pure ILs and the methanol + $[\mathrm{BMIM}^+][\mathrm{OcSO}_4^-]$ mixture together with reported data. The present experimental values of density for pure $[\mathrm{BMIM}^+][\mathrm{OcSO}_4^-]$ were compared with the data reported by other authors [9–12] and calculated with Tait EOS by Machida *et al.* [10] (see also Figures 1 and 2). The deviation statistics are: AAD = 0.14%, Bias = −0.19%, SD = 0.012%, SE = 0.004%, and Max. Dev. = 0.29%. No systematic deviations within 0.025–0.057% were found for the isotherms of 298 and 398 K, while for other measured isotherms of (323, 348, and 373 K) the deviations are systematically (our results are lower than calculated values) within 0.10–0.29%. The agreement between the present results and the values reported by Dávila *et al.* [11] for pure ILs is excellent (within 0.003–0.01%) at all measured temperatures and pressures. The single data point at room temperature (298 K) and at 0.1 MPa reported by Domańska *et al.* [9] is good (deviation is 0.12%) and agrees with the present results.

Figure 3 demonstrates the comparison between the present data for methanol + $[\mathrm{BMIM}^+][\mathrm{OcSO}_4^-]$ mixtures with the values reported by Domańska *et al.* [9]. Our interpolated data are agreed with the data by Domańska *et al.* [9] within 0.2%. As one can see from Figure 3, the densities of methanol + $[\mathrm{BMIM}^+][\mathrm{OcSO}_4^-]$ mixture changes rapidly at low concentration ranges (below 0.2 mole fraction of ILs, the slope of the $\rho - x$ curve is very steep), while at high concentrations of ILs the density slightly linear changes with concentration. The rate of the density changes is varied from 0 (at high concentrations) to 1150 kg m$^{-3}$ mol$^{-1}$ (at low concentrations).

Table 2. Experimental values of density, pressure, apparent molar volume, temperature and concentration of methanol + [BMIM$^+$][ OcSO$_4^-$ ] mixtures.

| $p$ (MPa) | $\rho$ (kg m$^{-3}$) | $V_\phi$ (cm$^3$ mol$^{-1}$) | $p$ (MPa) | $\rho$ (kg m$^{-3}$) | $V_\phi$ (cm$^3$ mol$^{-1}$) | $p$ (MPa) | $\rho$ (kg m$^{-3}$) | $V_\phi$ (cm$^3$ mol$^{-1}$) |
|---|---|---|---|---|---|---|---|---|
| Panel A: $x = 0.0$ (pure methanol)[a] | | | | $x = 0.0388$ | | | $x = 0.1351$ | |
| $T = 298.15$ K | | | | | | | | |
| 0.24 | 785.98 | – | 1.19 | 865.73 | 311.25 | 0.58 | 955.08 | 318.95 |
| 5.00 | 790.69 | – | 5.38 | 869.16 | 311.15 | 5.39 | 958.39 | 318.47 |
| 10.00 | 795.40 | – | 11.56 | 873.89 | 311.08 | 10.69 | 961.82 | 317.98 |
| 15.01 | 799.88 | – | 15.42 | 876.83 | 310.83 | 15.97 | 965.26 | 317.39 |
| 19.99 | 804.10 | – | 20.33 | 880.16 | 310.89 | 20.44 | 967.95 | 316.97 |
| 25.01 | 808.17 | – | 25.75 | 883.80 | 310.78 | 25.56 | 970.87 | 316.53 |
| 30.00 | 812.04 | – | 30.57 | 887.24 | 310.18 | 31.22 | 974.06 | 316.00 |
| 34.99 | 815.76 | – | 35.23 | 890.20 | 309.99 | 34.74 | 975.93 | 315.70 |
| 39.98 | 819.34 | – | 39.56 | 892.79 | 309.81 | 39.75 | 978.54 | 315.28 |
| $T = 323.15$ K | | | | | | | | |
| 0.27 | 762.14 | – | 1.03 | 843.45 | 314.73 | 1.03 | 936.98 | 322.24 |
| 4.99 | 767.53 | – | 5.41 | 847.36 | 315.00 | 5.08 | 939.90 | 321.97 |
| 9.98 | 772.87 | – | 10.03 | 851.32 | 315.15 | 10.61 | 943.73 | 321.56 |
| 14.98 | 777.91 | – | 15.47 | 855.79 | 315.15 | 15.09 | 946.69 | 321.22 |
| 19.99 | 782.69 | – | 20.31 | 859.57 | 315.12 | 20.41 | 950.05 | 320.81 |
| 24.99 | 787.21 | – | 25.19 | 863.21 | 315.07 | 25.09 | 952.85 | 320.47 |
| 30.00 | 791.53 | – | 30.51 | 866.98 | 315.02 | 30.74 | 956.05 | 320.09 |
| 34.99 | 795.64 | – | 35.62 | 870.40 | 315.03 | 35.12 | 958.39 | 319.83 |
| 39.99 | 799.60 | – | 39.97 | 873.16 | 315.10 | 39.97 | 960.84 | 319.56 |
| $T = 348.15$ K | | | | | | | | |
| 0.366 | 737.29 | – | 0.77 | 820.93 | 316.61 | 1.52 | 919.20 | 324.93 |
| 4.987 | 743.46 | – | 6.32 | 826.78 | 316.98 | 5.91 | 922.89 | 324.60 |
| 9.986 | 749.65 | – | 10.23 | 830.82 | 316.85 | 10.73 | 926.46 | 324.39 |
| 14.991 | 755.42 | – | 15.23 | 835.08 | 317.66 | 15.44 | 929.89 | 324.08 |
| 20.004 | 760.84 | – | 20.31 | 839.59 | 317.65 | 19.77 | 932.75 | 323.87 |
| 25.02 | 765.94 | – | 25.07 | 843.72 | 317.42 | 25.53 | 936.41 | 323.57 |
| 30.013 | 770.76 | – | 30.28 | 847.59 | 317.84 | 30.27 | 939.26 | 323.32 |
| 34.989 | 775.32 | – | 35.24 | 851.10 | 318.20 | 35.19 | 942.16 | 323.02 |
| 40.000 | 779.70 | – | 39.53 | 854.39 | 317.76 | 39.72 | 944.76 | 322.73 |
| $T = 373.15$ K | | | | | | | | |
| 0.534 | 710.55 | – | 2.04 | 800.53 | 314.52 | 1.08 | 901.34 | 326.17 |
| 4.983 | 717.67 | – | 5.74 | 804.93 | 315.43 | 5.07 | 904.88 | 326.25 |
| 9.99 | 724.99 | – | 10.03 | 809.80 | 316.09 | 10.06 | 909.13 | 326.17 |
| 14.998 | 731.69 | – | 15.21 | 815.36 | 316.55 | 15.21 | 913.30 | 325.98 |
| 19.985 | 737.88 | – | 20.64 | 820.81 | 316.83 | 20.08 | 917.06 | 325.72 |
| 24.994 | 743.68 | – | 25.91 | 825.73 | 317.06 | 25.09 | 920.72 | 325.44 |
| 29.997 | 749.13 | – | 30.46 | 829.69 | 317.31 | 30.14 | 924.22 | 325.14 |
| 35.001 | 754.27 | – | 35.72 | 833.93 | 317.71 | 35.09 | 927.44 | 324.87 |
| 39.996 | 759.14 | – | 39.38 | 836.66 | 317.99 | 39.94 | 930.42 | 324.63 |
| $T = 398.15$ K | | | | | | | | |
| 0.934 | 680.93 | – | 1.70 | 778.33 | 305.18 | 0.57 | 883.56 | 325.03 |
| 4.984 | 689.00 | – | 5.92 | 784.21 | 307.70 | 5.92 | 888.97 | 325.91 |
| 9.998 | 697.91 | – | 10.61 | 790.40 | 309.45 | 11.36 | 894.23 | 326.15 |
| 14.986 | 705.88 | – | 15.26 | 796.18 | 310.53 | 15.85 | 898.38 | 326.13 |
| 19.987 | 713.16 | – | 21.34 | 803.19 | 311.44 | 21.06 | 902.99 | 325.95 |

(*continued*)

Table 2. Continued.

| $p$ (MPa) | $\rho$ (kg m$^{-3}$) | $V_\phi$ (cm$^3$ mol$^{-1}$) | $p$ (MPa) | $\rho$ (kg m$^{-3}$) | $V_\phi$ (cm$^3$ mol$^{-1}$) | $p$ (MPa) | $\rho$ (kg m$^{-3}$) | $V_\phi$ (cm$^3$ mol$^{-1}$) |
|---|---|---|---|---|---|---|---|---|
| 24.992 | 719.87 | – | 26.08 | 808.24 | 311.99 | 25.86 | 907.03 | 325.69 |
| 29.991 | 726.11 | – | 30.05 | 812.19 | 312.42 | 30.31 | 910.61 | 325.41 |
| 35.005 | 731.99 | – | 35.22 | 816.93 | 313.11 | 36.23 | 915.12 | 325.00 |
| 40.004 | 737.47 | – | 40.08 | 820.99 | 313.90 | 39.76 | 917.66 | 324.77 |
| $x=0.2785$ | | | | $x=0.4961$ | | | $x=0.7497$ | |
| $T=298.15$ K | | | | | | | | |
| 0.32 | 1007.47 | 322.78 | 0.34 | 1040.32 | 324.91 | 0.45 | 1057.86 | 325.96 |
| 5.04 | 1010.37 | 322.16 | 5.03 | 1042.94 | 324.23 | 5.12 | 1060.31 | 325.25 |
| 10.23 | 1013.45 | 321.48 | 10.06 | 1045.68 | 323.51 | 10.34 | 1062.99 | 324.48 |
| 15.75 | 1016.60 | 320.78 | 15.12 | 1048.35 | 322.80 | 15.82 | 1065.72 | 323.70 |
| 20.64 | 1019.29 | 320.18 | 20.23 | 1050.96 | 322.11 | 20.03 | 1067.77 | 323.11 |
| 25.87 | 1022.04 | 319.57 | 25.06 | 1053.35 | 321.48 | 25.04 | 1070.16 | 322.42 |
| 30.32 | 1024.30 | 319.07 | 30.03 | 1055.73 | 320.86 | 30.12 | 1072.51 | 321.75 |
| 35.84 | 1026.98 | 318.47 | 35.07 | 1058.05 | 320.25 | 35.21 | 1074.80 | 321.09 |
| 39.96 | 1028.89 | 318.06 | 39.98 | 1060.24 | 319.67 | 39.93 | 1076.87 | 320.51 |
| $T=323.15$ K | | | | | | | | |
| 0.75 | 991.06 | 326.66 | 0.56 | 1024.37 | 329.34 | 0.56 | 1041.97 | 330.72 |
| 5.82 | 994.27 | 326.04 | 5.09 | 1027.02 | 328.66 | 5.02 | 1044.45 | 329.99 |
| 10.83 | 997.32 | 325.44 | 10.03 | 1029.80 | 327.94 | 10.08 | 1047.18 | 329.19 |
| 15.83 | 1000.24 | 324.84 | 15.05 | 1032.53 | 327.23 | 15.06 | 1049.78 | 328.43 |
| 20.98 | 1003.11 | 324.25 | 20.14 | 1035.20 | 326.53 | 20.21 | 1052.38 | 327.67 |
| 25.71 | 1005.62 | 323.74 | 25.09 | 1037.69 | 325.88 | 25.31 | 1054.87 | 326.94 |
| 30.73 | 1008.16 | 323.22 | 30.06 | 1040.08 | 325.25 | 30.06 | 1057.11 | 326.29 |
| 35.98 | 1010.68 | 322.71 | 35.92 | 1042.78 | 324.55 | 35.02 | 1059.36 | 325.63 |
| 39.95 | 1012.49 | 322.34 | 39.94 | 1044.55 | 324.09 | 39.98 | 1061.53 | 325.00 |
| $T=348.15$ K | | | | | | | | |
| 0.72 | 975.08 | 330.14 | 0.76 | 1009.49 | 333.41 | 0.98 | 1027.58 | 335.09 |
| 4.89 | 977.83 | 329.71 | 5.23 | 1012.10 | 332.78 | 4.92 | 1029.73 | 334.46 |
| 10.43 | 981.36 | 329.11 | 10.05 | 1014.84 | 332.10 | 10.03 | 1032.46 | 333.65 |
| 15.86 | 984.68 | 328.51 | 15.02 | 1017.58 | 331.40 | 15.21 | 1035.16 | 332.85 |
| 20.32 | 987.29 | 328.02 | 19.98 | 1020.24 | 330.72 | 19.98 | 1037.59 | 332.13 |
| 25.81 | 990.37 | 327.44 | 24.97 | 1022.84 | 330.05 | 25.03 | 1040.11 | 331.39 |
| 29.94 | 992.59 | 327.01 | 30.05 | 1025.39 | 329.39 | 30.09 | 1042.58 | 330.66 |
| 35.96 | 995.68 | 326.41 | 35.91 | 1028.24 | 328.64 | 35.02 | 1044.92 | 329.96 |
| 39.96 | 997.63 | 326.03 | 39.95 | 1030.13 | 328.15 | 39.98 | 1047.22 | 329.28 |
| $T=373.15$ K | | | | | | | | |
| 0.84 | 959.27 | 333.21 | 0.43 | 994.16 | 337.52 | 0.92 | 1012.72 | 339.67 |
| 4.92 | 962.23 | 332.85 | 5.06 | 997.08 | 336.86 | 5.08 | 1015.16 | 338.95 |
| 9.74 | 965.61 | 332.38 | 10.12 | 1000.20 | 336.12 | 10.12 | 1018.05 | 338.09 |
| 15.72 | 969.65 | 331.73 | 15.32 | 1003.31 | 335.35 | 14.89 | 1020.72 | 337.29 |
| 20.09 | 972.49 | 331.24 | 19.98 | 1006.02 | 334.67 | 20.12 | 1023.59 | 336.43 |
| 25.42 | 975.83 | 330.63 | 25.62 | 1009.22 | 333.84 | 25.02 | 1026.22 | 335.64 |
| 29.97 | 978.57 | 330.11 | 29.97 | 1011.61 | 333.22 | 30.12 | 1028.90 | 334.83 |
| 35.62 | 981.83 | 329.48 | 35.02 | 1014.31 | 332.51 | 35.03 | 1031.41 | 334.08 |
| 39.96 | 984.23 | 329.01 | 39.96 | 1016.87 | 331.83 | 39.97 | 1033.88 | 333.33 |
| $T=398.15$ K | | | | | | | | |
| 0.74 | 943.53 | 335.44 | 0.87 | 979.60 | 341.22 | 0.76 | 998.18 | 344.15 |

(*continued*)

Table 2. Continued.

| $p$ (MPa) | $\rho$ (kg m$^{-3}$) | $V_\phi$ (cm$^3$ mol$^{-1}$) | $p$ (MPa) | $\rho$ (kg m$^{-3}$) | $V_\phi$ (cm$^3$ mol$^{-1}$) | $p$ (MPa) | $\rho$ (kg m$^{-3}$) | $V_\phi$ (cm$^3$ mol$^{-1}$) |
|---|---|---|---|---|---|---|---|---|
| 5.07 | 947.05 | 335.24 | 5.32 | 982.70 | 340.59 | 4.92 | 1000.85 | 343.38 |
| 10.93 | 951.67 | 334.76 | 10.03 | 985.91 | 339.88 | 10.04 | 1004.06 | 342.43 |
| 15.72 | 955.33 | 334.26 | 15.05 | 989.25 | 339.09 | 15.09 | 1007.16 | 341.50 |
| 20.84 | 959.11 | 333.66 | 19.98 | 992.46 | 338.30 | 20.13 | 1010.18 | 340.59 |
| 25.74 | 962.63 | 333.04 | 25.03 | 995.66 | 337.48 | 25.07 | 1013.06 | 339.71 |
| 29.97 | 965.56 | 332.50 | 29.94 | 998.69 | 336.70 | 30.07 | 1015.91 | 338.84 |
| 35.21 | 969.09 | 331.81 | 35.62 | 1002.09 | 335.80 | 35.02 | 1018.66 | 338.00 |
| 39.19 | 971.68 | 331.29 | 39.95 | 1004.62 | 335.12 | 39.98 | 1021.35 | 337.18 |
| $x = 0.9312$ | | | $x = 1.0$ (pure [BMIM$^+$] [OcSO$_4^-$]) | | | | | |
| $T = 298.15$ K | | | | | | | | |
| 0.32 | 1065.12 | 326.42 | 0.29 | 1067.24 | – | | | |
| 5.02 | 1067.51 | 325.70 | 5.71 | 1069.98 | – | | | |
| 10.45 | 1070.22 | 324.88 | 10.52 | 1072.36 | – | | | |
| 15.32 | 1072.60 | 324.17 | 15.07 | 1074.57 | – | | | |
| 20.21 | 1074.94 | 323.47 | 20.13 | 1076.98 | – | | | |
| 25.32 | 1077.32 | 322.77 | 25.11 | 1079.30 | – | | | |
| 29.93 | 1079.43 | 322.14 | 30.40 | 1081.70 | – | | | |
| 35.02 | 1081.70 | 321.47 | 35.24 | 1083.85 | – | | | |
| 39.95 | 1083.85 | 320.84 | 40.01 | 1085.91 | – | | | |
| $T = 323.15$ K | | | | | | | | |
| 0.65 | 1049.36 | 331.27 | 0.28 | 1051.28 | – | | | |
| 5.03 | 1051.74 | 330.53 | 5.06 | 1053.88 | – | | | |
| 10.34 | 1054.54 | 329.67 | 10.21 | 1056.60 | – | | | |
| 15.92 | 1057.39 | 328.80 | 15.64 | 1059.37 | – | | | |
| 20.43 | 1059.63 | 328.11 | 20.03 | 1061.55 | – | | | |
| 25.83 | 1062.23 | 327.32 | 25.08 | 1063.98 | – | | | |
| 30.32 | 1064.32 | 326.68 | 30.18 | 1066.35 | – | | | |
| 35.73 | 1066.76 | 325.95 | 35.34 | 1068.67 | – | | | |
| 39.94 | 1068.60 | 325.39 | 39.94 | 1070.67 | – | | | |
| $T = 348.15$ K | | | | | | | | |
| 0.32 | 1034.68 | 335.91 | 0.48 | 1036.91 | – | | | |
| 5.02 | 1037.16 | 335.12 | 6.34 | 1039.98 | – | | | |
| 10.32 | 1039.92 | 334.25 | 10.35 | 1042.05 | – | | | |
| 15.84 | 1042.73 | 333.37 | 15.72 | 1044.77 | – | | | |
| 20.65 | 1045.12 | 332.62 | 21.53 | 1047.66 | – | | | |
| 25.62 | 1047.56 | 331.86 | 25.99 | 1049.84 | – | | | |
| 29.95 | 1049.64 | 331.21 | 30.61 | 1052.06 | – | | | |
| 35.92 | 1052.45 | 330.34 | 36.07 | 1054.63 | – | | | |
| 39.96 | 1054.31 | 329.77 | 39.95 | 1056.43 | – | | | |
| $T = 373.15$ K | | | | | | | | |
| 0.76 | 1020.19 | 340.61 | 0.11 | 1022.04 | – | | | |
| 5.62 | 1022.93 | 339.72 | 5.95 | 1025.31 | – | | | |
| 10.43 | 1025.60 | 338.86 | 10.82 | 1027.98 | – | | | |
| 15.23 | 1028.22 | 338.01 | 15.34 | 1030.41 | – | | | |
| 20.54 | 1031.05 | 337.11 | 20.73 | 1033.26 | – | | | |
| 25.31 | 1033.55 | 336.31 | 25.58 | 1035.77 | – | | | |
| 29.94 | 1035.92 | 335.55 | 30.85 | 1038.45 | – | | | |

(*continued*)

Table 2. Continued.

| $p$ (MPa) | $\rho$ (kg m$^{-3}$) | $V_\phi$ (cm$^3$ mol$^{-1}$) | $p$ (MPa) | $\rho$ (kg m$^{-3}$) | $V_\phi$ (cm$^3$ mol$^{-1}$) | $p$ (MPa) | $\rho$ (kg m$^{-3}$) | $V_\phi$ (cm$^3$ mol$^{-1}$) |
|---|---|---|---|---|---|---|---|---|
| 35.06 | 1038.50 | 334.73 | 36.22 | 1041.11 | – | | | |
| 39.97 | 1040.91 | 333.97 | 40.01 | 1042.96 | – | | | |
| $T = 398.15$ K | | | | | | | | |
| 0.87 | 1005.97 | 345.32 | 0.33 | 1007.09 | – | | | |
| 5.21 | 1008.65 | 344.44 | 6.18 | 1011.44 | – | | | |
| 10.32 | 1011.74 | 343.42 | 10.81 | 1014.19 | – | | | |
| 15.92 | 1015.04 | 342.33 | 15.66 | 1017.00 | – | | | |
| 20.43 | 1017.63 | 341.48 | 21.15 | 1020.12 | – | | | |
| 25.84 | 1020.67 | 340.49 | 25.48 | 1022.53 | – | | | |
| 30.43 | 1023.19 | 339.67 | 30.95 | 1025.51 | – | | | |
| 35.92 | 1026.12 | 338.71 | 35.97 | 1028.18 | – | | | |
| 39.95 | 1028.22 | 338.03 | 40.03 | 1030.29 | – | | | |

Note: [a]Ihmels *et al.* [18].

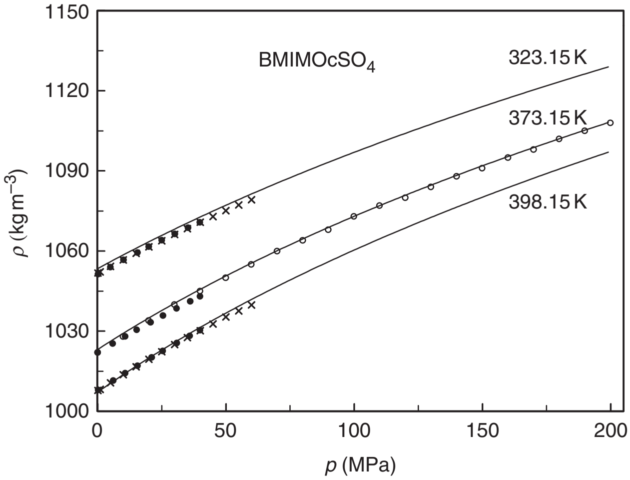

Figure 1. Measured values of density of pure [BMIM$^+$][OcSO$_4^-$] as a function of pressure along three selected isotherms together with reported data and the values calculated from EOS by Machida *et al.* [10]. ●, this work; ○, Machida *et al.* [10] (exp.); ×, Dávila *et al.* [11]; (———), Machida *et al.* [10] (cal.).

### 3.2. *Excess molar volumes*

The excess molar volumes for the methanol + [BMIM$^+$][OcSO$_4^-$] mixtures were calculated using the present measured molar volumes for the mixtures and pure ILs and the values of molar volumes for pure methanol calculated from IUPAC [19] fundamental (EOS) with the following relation

$$V_{\mathrm{m}}^{\mathrm{E}}(p,T,x) = V_{\mathrm{m}}(p,T,x) - xV_1(p,T,1) - (1-x)V_2(p,T,0), \tag{3}$$

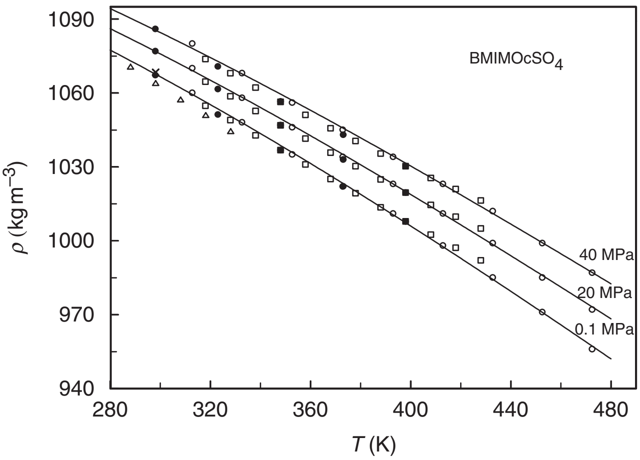

Figure 2. Measured values of density of pure $[BMIM^+][OcSO_4^-]$ as a function of temperature along various selected isobars together with reported data and the values calculated from EOS by Machida *et al.* [10]. ●, this work; ○, Machida *et al.* [10] (exp.); □, Dávila *et al.* [11]; ×, Domańska *et al.* [9]; Δ, Wandschneider *et al.* [12]; (———), Machida *et al.* [10] (cal.).

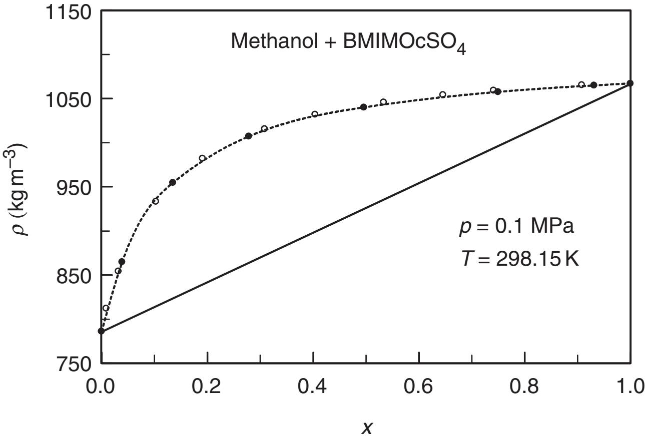

Figure 3. Measured values of density of methanol + $[BMIM^+][OcSO_4^-]$ mixtures as a function of molarity at atmospheric pressure together with data reported by Domańska *et al.* [9] and calculated from Tait EOS (6). ●, this work; ○, Domańska *et al.* [9]; (– – – –), Tait EOS (6). The solid line is the ideal mixture.

where $x$ is the mole fraction of $[BMIM^+][OcSO_4^-]$, $V_m(p, T, x)$ is the experimentally determined molar volumes of the mixture of concentration $x$ at temperature $T$ and pressure $p$, and $V_1 = V_m(p, T, 1)$ and $V_2 = V_m(p, T, 0)$ are the molar volumes of the pure components at the same pressure $p$ and temperature $T$. The derived values of $V_m^E$ for the selected temperature of 323.15 K and various pressures are presented in Table 3 and shown in Figure 4 as a function of mole fraction $x$ of ILs. The maximum relative uncertainty, $\delta V_m^E$, in the derived values of $V_m^E$ is about 5–10% depending on

Table 3. Excess and partial molar volumes for methanol+[BMIM$^+$][OcSO$_4^-$] mixtures derived from the present density measurements.

| $x$ | $p=0.1$ MPa | | $p=10$ MPa | | $p=20$ MPa | | $p=30$ MPa | | $p=40$ MPa | |
|---|---|---|---|---|---|---|---|---|---|---|
| | $V_m^E$ (cm$^3$ mol$^{-1}$) | | $V_m^E$ (cm$^3$ mol$^{-1}$) | | $V_m^E$ (cm$^3$ mol$^{-1}$) | | $V_m^E$ (cm$^3$ mol$^{-1}$) | | $V_m^E$ (cm$^3$ mol$^{-1}$) | |
| $T=323.15$ K | | | | | | | | | | |
| 0.0 | 0.0 | | 0.0 | | 0.0 | | 0.0 | | 0.0 | |
| 0.0388 | −0.6860 | | −0.5931 | | −0.5152 | | −0.4526 | | −0.3993 | |
| 0.1351 | −1.2752 | | −1.1370 | | −1.0123 | | −0.9011 | | −0.7979 | |
| 0.2785 | −1.3591 | | −1.2258 | | −1.1017 | | −0.9870 | | −0.8771 | |
| 0.4961 | −1.0731 | | −0.9710 | | −0.8768 | | −0.7861 | | −0.7031 | |
| 0.7497 | −0.5657 | | −0.5112 | | −0.4618 | | −0.4154 | | −0.3735 | |
| 0.9312 | −0.1660 | | −0.1412 | | −0.1266 | | −0.1130 | | −0.1098 | |
| 1.0 | 0.0 | | 0.0 | | 0.0 | | 0.0 | | 0.0 | |
| | $\bar{V}_1$ | $\bar{V}_2$ | $\bar{V}_1$ | $\bar{V}_2$ | $\bar{V}_1$ | $\bar{V}_2$ | $\bar{V}_1$ | $\bar{V}_2$ | $\bar{V}_1$ | $\bar{V}_2$ |
| $T=323.15$ K | | | | | | | | | | |
| 0.0 | 42.05 | 324.42 | 41.46 | 323.44 | 40.94 | 322.52 | 40.48 | 321.68 | 40.08 | 320.90 |
| 0.0388 | 41.62 | 324.60 | 41.10 | 323.64 | 40.63 | 322.72 | 40.21 | 321.86 | 39.84 | 321.06 |
| 0.1351 | 41.45 | 325.97 | 40.93 | 324.86 | 40.47 | 323.80 | 40.07 | 322.83 | 39.72 | 321.92 |
| 0.2785 | 41.43 | 328.26 | 40.91 | 326.90 | 40.44 | 325.63 | 40.04 | 324.45 | 39.69 | 323.37 |
| 0.4961 | 40.58 | 330.88 | 40.14 | 329.27 | 39.75 | 327.75 | 39.42 | 326.35 | 39.13 | 325.04 |
| 0.7497 | 37.84 | 332.19 | 37.67 | 330.46 | 37.54 | 328.83 | 37.45 | 327.31 | 37.39 | 325.90 |
| 0.9312 | 34.65 | 331.91 | 34.81 | 330.21 | 34.98 | 328.61 | 35.17 | 327.12 | 35.36 | 325.73 |
| 1.0 | 33.18 | 331.54 | 33.48 | 329.88 | 33.79 | 328.31 | 34.10 | 326.85 | 34.42 | 325.50 |

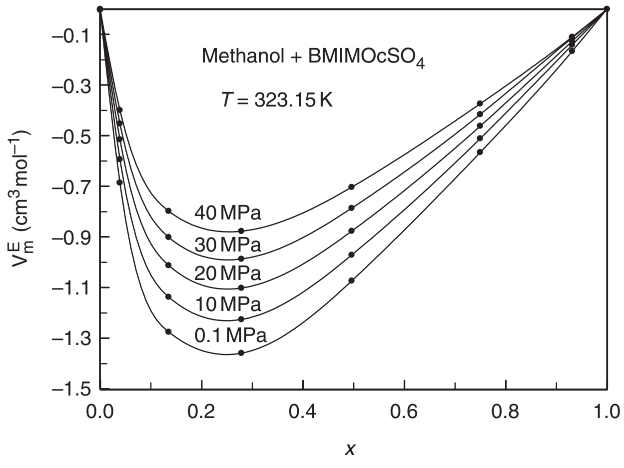

Figure 4. Excess molar volumes $V_m^E$ of methanol + [BMIM$^+$][OcSO$_4^-$] mixtures as a function of concentration $x$ for selected isobars and at selected temperature of 323.15 K.

the temperature, pressure, and concentration. At concentrations close to the pure components, the uncertainty in $V_m^E$ increases from 20 to 30% and more. Note that the values of $V_m^E$ for the methanol + [BMIM$^+$][OcSO$_4^-$] mixtures are negative for all measured temperatures and pressures over the whole composition range. This means that the measured mixture molar volumes $V_m$ are less than the ideal mixture molar volume $V_{id} = xV_1 + (1 - x)V_2$. Therefore, the addition of the IL molecules to methanol changes the spatial microstructure of methanol surrounding the IL ions i.e. local environment (microstructure) around an IL solute changes in comparison with the ideal mixture or bulk microstructure. Therefore, methanol + $[BMIM^+][OcSO_4^-]$ mixtures exhibit 'attractive' behaviour (Krichevskii function for this mixture is also negative, i.e. addition of small amount of ILs into the methanol at constant $T$ and $V$ decreases the pressure of the system, see Section 3.5). This means that when adding the IL ions to methanol the local density (also local structure around the IL ions changes) of methanol molecules around IL ions increases (molar volume decreases) compared with the ideal mixture or bulk density of pure methanol. Thus, the addition of methanol to $[BMIM^+][OcSO_4^-]$ may result in changes in topology of the methanol molecules or $[BMIM^+][OcSO_4^-]$ ions. This 'packing effect' caused a decrease in the molar volume of the mixture in comparison with the ideal mixture. Therefore, the excess molar volume behaviour depends on microscopic phenomena involving local structure perturbations induced by the presence of the solute (IL) ions.

As one can see from Figure 4, the $V_m^E$–$x$ curves of excess molar volumes of methanol + $[BMIM^+][OcSO_4^-]$ mixtures are noticeably skewed towards a low mole fraction of $[BMIM^+][OcSO_4^-]$ ($V_m^E$–$x$ curves are highly asymmetric). This behaviour of the $V_m^E$ is typical for alcohol + ILs mixtures (Abdulagatov *et al.* [13–15]). The excess molar volume minimum is found at a concentration of about 0.3 mole fraction of $[BMIM^+][OcSO_4^-]$. The same trend was also found [21] in $V_m^E$ for IL mixtures containing organic solutes (alcohols). This can be attributed partly to the large differences in the size and shapes of the ions ($[BMIM^+]$ and $[OcSO_4^-]$) and methanol molecules. The pressure decreases (absolute values) for the excess molar volumes.

Figure 5 compares the derived values of excess molar volumes for methanol + $[BMIM^+][OcSO_4^-]$ mixtures with the values reported by Domańska *et al.* [9]. The differences are very large (up to 45%), although the differences between the present measured molar volumes and reported by Domańska *et al.* [9] are within 0.2%. This is because the magnitude of the $V_m^E$ is small and the uncertainty of the $V_m^E$ is large, $\delta V_m^E \cong (V_m - V_{id})^{-1}$ [22,23], due to the small difference between $V_m$ and $V_{id}$, $(V_m - V_{id}) \to 0$.

Figure 6(a) shows the concentration dependence of the excess molar volumes of a series of methanol-containing binary mixtures with the same first component (methanol) and various second components (organic solvents, other ILs and water) at a selected temperature of 298.15 K and at 0.1 MPa. This figure demonstrates the effect of the nature of the second component on the values and concentration dependence behaviour of the excess molar volumes of methanol-containing binary mixtures. As one can see from Figure 6(a), the introduction of various ILs and other organic solvent or water differntly changes concentration dependence of $V_m^E$. For example, *n*-pentane and $C_2H_5I$ positively changes the concentration dependence of $V_m^E$, while all of the ILs and water negative changes the concentration dependence of $V_m^E$. For methanol + toluene mixture, the values of $V_m^E$ is very small (negative). $V_m^E - x$ dependence on the methanol + water mixture is symmetric, while for methanol + ILs mixture is asymmetric. The location of the minimum of $V_m^E - x$ curve for all studied methanol + ILs is almost the same (between 0.2 and 0.3 mole fraction of ILs). Figure 6(b) shows that putting alcohols (starting with butanol) into the ILs ($[BMIM^+][OcSO_4^-]$) structure results in considerable

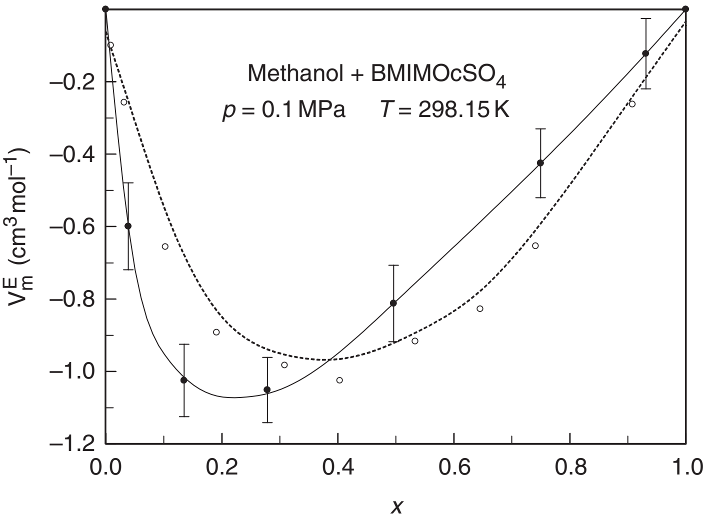

Figure 5. Comparison of excess molar volumes $V_m^E$ of methanol + [BMIM$^+$][OcSO$_4^-$] with the values reported by Domańska *et al.* [9] at atmospheric pressure and at temperature of 298.15 K. ●, this work; ○, Domańska *et al.* [9]; (———), smoothed curves; (··········), smoothed curves for the data by Domańska *et al.* [9].

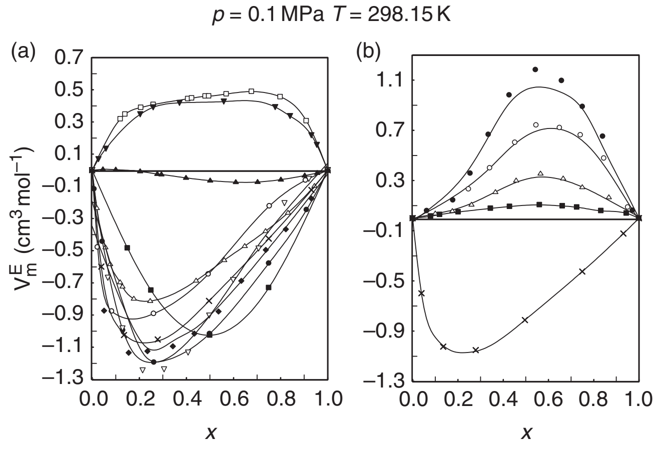

Figure 6. Comparison of excess molar volumes $V_m^E$ of methanol-containing (a) and [BMIM$^+$][OcSO$_4^-$]-containing (b) binary mixtures as a function of concentration $x$ at 1 MPa and 298.15 K together with the present results for methanol + [BMIM$^+$][OcSO$_4^-$]. (a): ●, this work (methanol + [BMIM$^+$][OcSO$_4^-$]); ○, Abdulagatov *et al.* [15] (methanol + [BMIM+][$BF_4^-$]); ×, Abdulagatov *et al.* [14] (methanol + [BMIM+][$PF_6^-$]); Δ, González *et al.* [24] (methanol + $C_8$MIMCl); ■, Magee and Abdulagatov [27] (methanol + water); □, Atik [25] (methanol + $C_2H_5I$) [11]; ▲, Rodriguez *et al.* [28] (methanol + toluene); ▼, Ore *et al.* [26] (methanol + *n*-pentane); ∇, Domańska *et al.* [9] (methanol + [MMIM$^+$][$CH_3SO_4^-$]); ◆, Domańska *et al.* [9] (methanol + [BMIM$^+$][$CH_3SO_4^-$]); (b): ●, Domańska *et al.* [9] (decanol + [BMIM$^+$][OcSO$_4^-$]); ○, Domańska *et al.* [9] (octanol + [BMIM$^+$][OcSO$_4^-$]); ×, this work (methanol + [BMIM$^+$][OcSO$_4^-$]); Δ, Domańska *et al.* [9] (hexanol + [BMIM$^+$][OcSO$_4^-$]); ■, Domańska *et al.* [9] (butanol + [BMIM$^+$][OcSO$_4^-$]).

increases in the excess molar volumes to more positive values, while methanol negatively changes the $V_m^E$ values.

### 3.3. *Apparent molar volumes*

The measured densities for methanol + [BMIM$^+$][OcSO$_4^-$] mixtures were also used to calculate the apparent molar volumes, $V_\phi$, of [BMIM$^+$][OcSO$_4^-$] in methanol using the well-known relation

$$V_\phi = (\rho_0 - \rho_S)/(m\rho_S\rho_0) + M/\rho_S, \tag{4}$$

where $\rho_0$ and $\rho_S$ are densities of pure methanol (calculated with IUPAC accepted fundamental EOS [19]) and the present results for the mixture, respectively, $m$ is the molality of mixture, and $M$ is the molar mass of the dissolved ILs. The derived values of the apparent molar volumes are given in Table 2 at each measured $T$ and $p$ and shown in Figures 7 and 8 in the $V_\phi - m$ and $V_\phi - T$ projections for the various selected concentrations and pressures. The maximum relative uncertainty of the derived values of apparent molar volumes, $\delta V_\phi$, is about $\delta V_\phi = 0.15\%$ at high concentrations and 1–2% at low concentrations. The sharp changes of $V_\phi$ at low molalities (below 50 mol kg$^{-1}$) is found, while at high molalities $V_\phi$ is almost constant. As Figure 8 shows, at low concentrations of ILs (below 0.28 mole fraction), $V_\phi - T$ dependence goes through the maximum at temperatures around 350 K. As the concentration of ILs increases the maximum becomes less pronounced, at concentrations of about 0.28 mole fraction the maximum is vanished. Above 0.28 mole fraction $V_\phi$ almost linearly increases with increase in temperature. For the dilute mixtures the maximum of $V_\phi - T$ is more markedly exhibited.

Derived apparent molar volumes were fitted to the Pitzer's ion-interaction relation [29] to accurately calculate the values of apparent molar volumes at infinite dilution, $V_\phi^0$

$$V_\phi = V_\phi^0 + \nu|z_M z_X| A_V h(I) + 2\nu_M z_M RT\left[mB_{MX}^V + m^2(\nu_M \nu_X)C_{MX}^V\right], \tag{5}$$

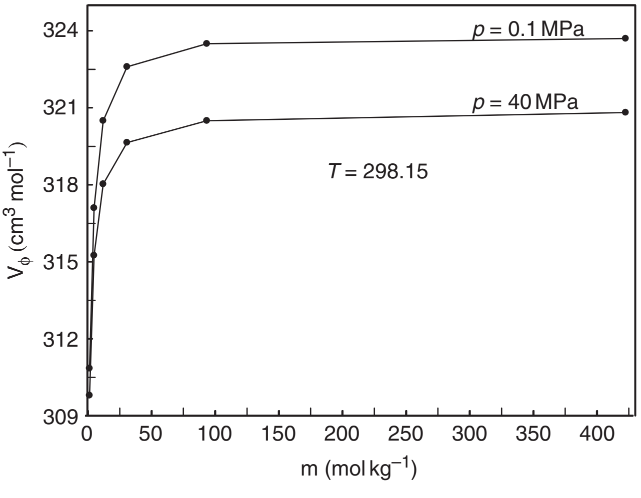

Figure 7. Apparent molar volumes $V_\phi$ of [BMIM$^+$][OcSO$_4^-$] in methanol as a function of molality $m$ for a selected isotherm of 298.15 K and at two isobars 0.1 and 40 MPa.

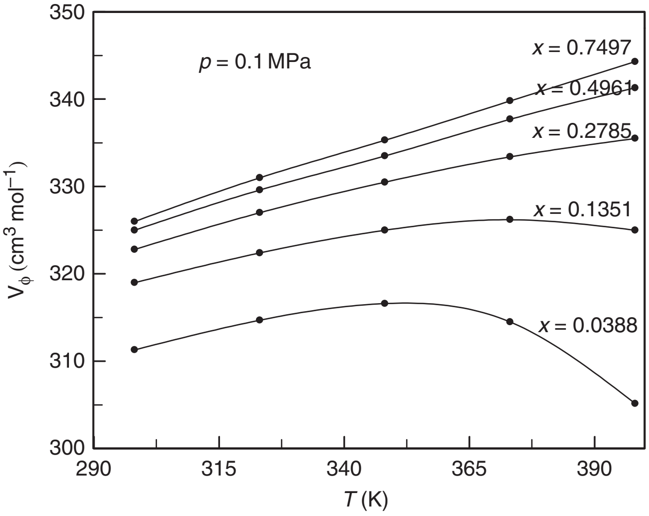

Figure 8. Apparent molar volumes $V_\phi$ of [BMIM$^+$][OcSO$_4^-$] in methanol as a function of temperature $T$ at atmospheric pressure for various compositions.

where $h(I) = \ln(1 + bI^{1/2})/2b$, $A_V = -4RT(\partial A_\phi/\partial p)_T$, $C_{MX} = C^\phi_{MX}/2|z_M z_X|^{1/2}$, $B_{MX} = \beta^0_{MX} + 2\beta^1_{MX}[1-(1+\alpha I^{1/2})\exp(-\alpha I^{1/2})]/\alpha^2 I$, $B^V_{MX}(I) = (\partial B_{MX}/\partial p)_{T,I}$, $C^V_{MX} = (\partial C_{MX}/\partial p)_T$, $I = 0.5\sum_i m_i z_i^2$, where $A_V$ and $A_\phi$ are the Debye–Huckel slope for the apparent molar volume and osmotic coefficient, respectively, $b = 1.2$ (kg mol$^{-1}$)$^{1/2}$, $R = 8.3145$ J mol$^{-1}$ K$^{-1}$, $B_{MX}$ and $C_{MX}$ are the second and third virial coefficients, $I$ is the ionic strength, $z_i$ are the charges of the ions, and $\alpha \approx 2$ kg$^{1/2}$ mol$^{-1/2}$ is the ion-interaction parameter specific to each solute (may be adjusted for each solute) and might remain the same for broad classes of solutes [29,30]. Pitzer's Equation (5) describes quite well (standard deviations for each isotherm–isobar are varied within $0.5 \times 10^{-6}$–$1.0 \times 10^{-6}$) the present apparent molar volumes data over a wide range of temperature, pressure, and concentration, if it is assumed that the coefficients $\beta^{(0)}$, $\beta^{(1)}$, and $C^v$ are functions of pressure and temperature. As a rule, Equation (5) is applied at fixed pressure $p$ and temperature $T$. The derived parameter values of Pitzer's model for selected fixed temperatures and pressures are given in Table 4. The infinite-dilution values of $V_\phi$ (or partial molar volumes $\bar{V}^0_2$) as a function of temperature are depicted in Figure 9 (see also Table 5) along three selected pressures (0.1, 20 and 40 MPa). Note that $V^0_\phi$ (Figure 9) are passing through the maximum-like $V_\phi$ at low concentrations (Figure 8) at temperatures about 350 K and then rapidly decrease with increasing temperature (and probably goes to negative values at high temperatures, especially at low pressures, like most aqueous solutions [31,32]). At high pressure (about 40 MPa), the maximum of the $V^0_\phi - T$ dependence is less pronounced than at low pressures.

### 3.4. *Equation of state (EOS)*

The present measured densities for methanol + [BMIM$^+$][OcSO$_4^-$] mixtures were used to develop a Tait-type EOS which has been previously successfully applied by many authors for pure fluids and mixtures [10,11,33–41].

Table 4. Parameters of the Pitzer's ion-interaction model for methanol + [BMIM$^+$][OcSO$_4^-$] (Equation (5)), as a function of temperature and pressure.

| $T$ (K) | $V_\phi^0$ (cm$^3$ mol$^{-1}$) | $A_V$ (mol$^{-1}$ kg)$^{1/2}$ | $-10^3 \times B_{MX}^V$ (kg mol$^{-1}$ MPa$^{-1}$) | $10^7 \times C_{MX}^V$ (kg$^2$ mol$^{-2}$ MPa$^{-1}$) |
|---|---|---|---|---|
| $p = 0.1$ MPa | | | | |
| 298.15 | 298.68 | 18.799 | 0.0319 | 0.4943 |
| 323.15 | 301.10 | 19.942 | 0.0288 | 0.4326 |
| 348.15 | 301.20 | 22.449 | 0.0290 | 0.4347 |
| 373.15 | 293.32 | 30.902 | 0.0383 | 0.5769 |
| 398.15 | 271.69 | 49.421 | 0.0611 | 0.9366 |
| $p = 20$ MPa | | | | |
| 298.15 | 300.13 | 15.793 | 0.0255 | 0.3878 |
| 323.15 | 304.81 | 15.099 | 0.0210 | 0.3184 |
| 348.15 | 305.94 | 16.968 | 0.0214 | 0.3231 |
| 373.15 | 300.73 | 23.439 | 0.0278 | 0.4180 |
| 398.15 | 286.01 | 37.013 | 0.0456 | 0.0170 |
| $p = 40$ MPa | | | | |
| 298.15 | 300.83 | 13.320 | 0.0217 | 0.3332 |
| 323.15 | 307.08 | 11.726 | 0.0160 | 0.2395 |
| 348.15 | 308.37 | 13.548 | 0.0168 | 0.2487 |
| 373.15 | 305.57 | 18.014 | 0.0213 | 0.3198 |
| 398.15 | 294.58 | 28.276 | 0.0329 | 0.4985 |

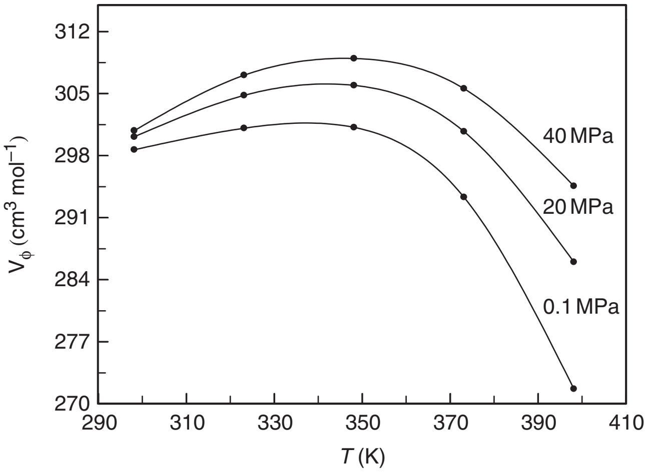

Figure 9. Apparent molar volumes at infinite dilution $V_\phi^0$ of [BMIM$^+$][OcSO$_4^-$] in methanol as a function of temperature, $T$, for three selected isobars of 0.1, 20, and 40 MPa.

$$\frac{\rho - \rho_0}{\rho_0} = c \log\left(\frac{B + p}{B + p_0}\right). \tag{6}$$

For the pure components, parameter $c$ is a constant, $B_i = b_{1i} + b_{2i}T$ ($i = 1$ for [BMIM$^+$][OcSO$_4^-$] and $i = 2$ for pure methanol) is a linear function of temperature, $\rho_0$ is

Table 5. Apparent molar volume of $[BMIM^+][OcSO_4^-]$ in methanol at infinite dilution as a function of temperature at three selected pressures.

| $T$ (K) | $V_\phi^0$ (cm$^3$ mol$^{-1}$) |
|---|---|
| $p=0.1$ MPa | |
| 298.15 | 298.68 |
| 323.15 | 301.10 |
| 348.15 | 301.20 |
| 373.15 | 293.32 |
| 398.15 | 271.69 |
| $p=20$ MPa | |
| 298.15 | 300.13 |
| 323.15 | 304.81 |
| 348.15 | 305.94 |
| 373.15 | 300.73 |
| 398.15 | 286.01 |
| $p=40$ MPa | |
| 298.15 | 300.83 |
| 323.15 | 307.08 |
| 348.15 | 308.37 |
| 373.15 | 305.57 |
| 398.15 | 294.58 |

Table 6. Values of the Tait EOS parameters for pure $[BMIM^+][OcSO_4^-]$ and methanol together with values for their mixture.

| $[BMIM^+][OcSO_4^-]$, AAD = 0.016%<br>$b_{ij}$ | $c_{ij}$ |
|---|---|
| $b_{11}=394.5758$ | $c_1=0.11291$ |
| $b_{21}=-0.52514$ | – |
| Methanol, AAD = 0.052% | |
| $b_{12}=272.4984$ | $c_2=0.13$ |
| $b_{22}=-0.57666$ | – |
| Methanol + $[BMIM^+][OcSO_4^-]$, AAD = 0.187% | |
| $b_{1m}=713.8158$ | $c_{1m}=-1.357795$ |
| $b_{2m}=-3.07683$ | $c_{2m}=5.152895$ |
| $b_{3m}=10197.2032$ | |

the density of liquid at pressure $p_0$ (usually $p_0=0.1$ MPa). The parameter $B$ in the Tait EOS is related to the intermolecular interaction. The derived values of parameters of the Tait EOS (6) for pure components ($[BMIM^+][OcSO_4^-]$ and methanol) are given in Table 6. The uncertainty of the representation of the present experimental data is 0.052 and 0.016%

for pure methanol and pure $[\mathrm{BMIM}^+][\mathrm{OcSO}_4^-]$, respectively. The measured mixture densities at atmospheric pressure were fitted to the equation

$$\rho_0(T,x,p=0.1) = x\rho_{01} + (1-x)\rho_{02} + x(1-x)\left[A_1 + A_4T^3 + A_2(1-x)^2 + A_3(1-x)^9\right], \tag{7}$$

where $\rho_{01}(T, x=1, p_0=0.1)$ and $\rho_{02}(T, x=0, p_0=0.1)$ are the densities of pure components, $[\mathrm{BMIM}^+][\mathrm{OcSO}_4^-]$ and methanol, respectively, at atmospheric pressure as a function of temperature, $A_1=164.0385$, $A_2=765.0324$, $A_3=1346.6943$ and $A_4=0.315\times10^{-5}$ are fitting parameters. To accurately represent measured densities of pure components at atmospheric pressure, the following quadratic functions were used

$$\rho_{01}(T, x=1, p=0.1) = 1285.741 - 0.8401T + 3.5689\times10^{-4}T^2, \tag{8}$$

$$\rho_{02}(T, x=0, p=0.1) = 893.6835 + 0.1582T - 0.1746\times10^{-2}T^2. \tag{9}$$

The value of thermal expansion coefficient, $\alpha=(1/\rho)(\partial\rho/\partial T)_p$, calculated with Equation (8) for ILs at temperature 300 K and at 0.1 MPa ($5.873\times10^{-4}\,\mathrm{K}^{-1}$) is good (within 5%); this agrees with the value reported by Wandschneider [12] and Dávila *et al.* [11], while the value reported by Machida *et al.* [10] agrees within 13%. Equation (7) reproduces the present density data for methanol + $[\mathrm{BMIM}^+][\mathrm{OcSO}_4^-]$ mixture at atmospheric pressure and at any temperatures between 298 and 398 K and in the whole concentration range within 0.23%. In the present work, Equation (6) was applied to the methanol + $[\mathrm{BMIM}^+][\mathrm{OcSO}_4^-]$ mixture. This equation was successfully used in our previous papers (Abdulagatov *et al.* [13–15]) to accurately represent the density measurements for three ILs containing binary mixtures (ethanol + $\mathrm{BMIMBF}_4$, methanol + $\mathrm{BMIMBF}_4$ and methanol + $\mathrm{BMIMPF}_6$). The Tait-type EOS was also very carefully studied in other research (see for example, [10,11,33–40]) and was applied for pure fluids and fluid mixtures and recommended to be used for the representation of experimental density data in the liquid phase. Recently Hofman *et al.* [41] used the Tait EOS to represent the experimental densities for methanol + $\mathrm{C_2MIMEtSO_4}$ mixture. Gu and Brennecke [33] also successfully used the Tait model to represent high-pressure density measurements for ILs with an accuracy of 0.08–0.3%. The structure of the temperature $B(T)$ and concentration $c(x)$ functions in the Tait Equation (6) for the mixture was optimised. For the mixture methanol + $[\mathrm{BMIM}^+][\mathrm{OcSO}_4^-]$, the best result was achieved for the functions

$$B_m = xB_1 + (1-x)B_2 + x(1-x)\left(b_{1m} + b_{2m}T + b_{3m}x^2\right), \tag{10}$$

$$c_m = xc_1 + (1-x)c_2 + x(1-x)(c_{1m} + c_{2m}x). \tag{11}$$

The derived values of the adjusting parameters of Equations (10) and (11) and AAD for the mixture are given in Table 6, together with the values for pure component. As one can see from this table, the AAD for the mixture is 0.187% in the entire concentration range and at temperatures from 298 to 398 K and up to 40 MPa. In total, Equation (6) contains minimal (five) adjustable coefficients for the mixture. Figure 10 shows the deviation plot (percentage relative deviations) between the present measured densities and the values calculated with Equation (6) for the methanol + $[\mathrm{BMIM}^+][\mathrm{OcSO}_4^-]$ mixture. An equation of state (6) was used to calculate some derived thermodynamic and structural properties of

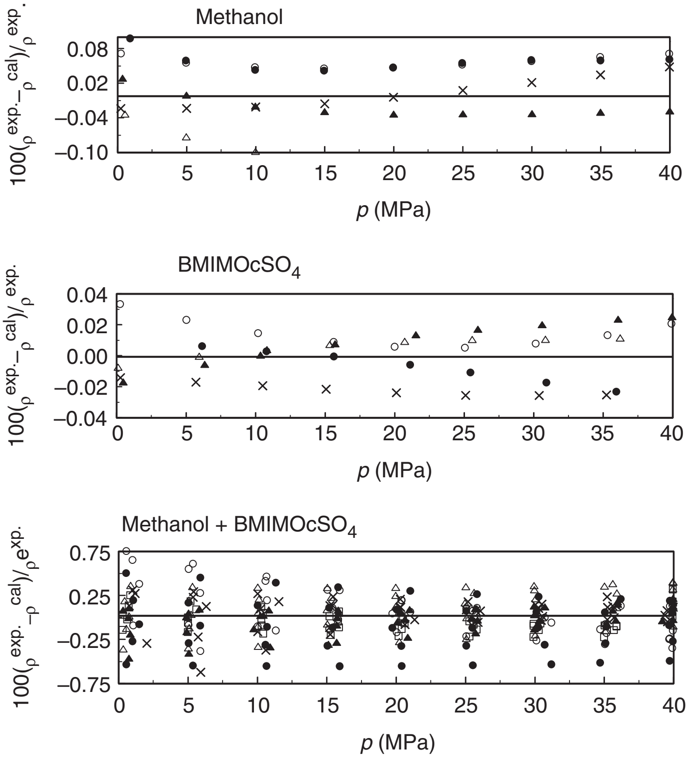

Figure 10. Percentage deviations, $\delta\rho = 100(\rho^{\text{exp}} - \rho^{\text{cal}}/\rho^{\text{exp}})$ of the present experimental densities for pure methanol, [BMIM$^+$][OcSO$_4^-$], and their mixtures from the values calculated with the Tait EOS (Equation (6)): Methanol and [BMIM$^+$][OcSO$_4^-$]: ●, 298.15 K; ○, 323.15 K; ▲, 348.15 K; Δ, 373.15 K; ×, 398.15 K; Methanol + [BMIM$^+$][OcSO$_4^-$]: ×, $x = 0.0388$; ○, $x = 0.1351$; ▲, $x = 0.2785$; Δ, $x = 0.4961$; ●, $x = 0.7497$; □, $x = 0.9312$.

the methanol + [BMIM$^+$][OcSO$_4^-$] mixture, such as partial molar volumes, direct and total correlation function integrals and the Krichevskii function (Section 3.5).

### 3.5. *Partial molar volume and structural properties of dilute mixtures of methanol + [BMIM$^+$][OcSO$_4^-$]*

The partial molar volumes $\overline{V}_i$, $i+1, 2$, can be obtained from the slope of the tangent $(\partial V_{\text{m}}/\partial x)_{pT}$ as

$$\overline{V}_1 = V_{\text{m}} - x\left(\frac{\partial V_{\text{m}}}{\partial x}\right)_{p,T}, \quad \overline{V}_2 = V_{\text{m}} + (1-x)\left(\frac{\partial V_{\text{m}}}{\partial x}\right)_{p,T}, \tag{12}$$

using the measured values of molar volumes for the mixture $V_{\text{m}}$. The concentration derivatives $(\partial V_{\text{m}}/\partial x)_{pT}$ were calculated with the Tait EOS (6) for the mixture. Derived values of the partial molar volumes for the selected isotherm of 323.15 K at various pressures are given in Table 3. Figure 11 shows the concentration dependence of the partial molar volumes, $\overline{V}_i$, calculated with Equation (12) using the present molar volume data. As Figure 11(a) shows, each $\overline{V}_1 - x$ isotherm–isobar has a minimum at a low concentration

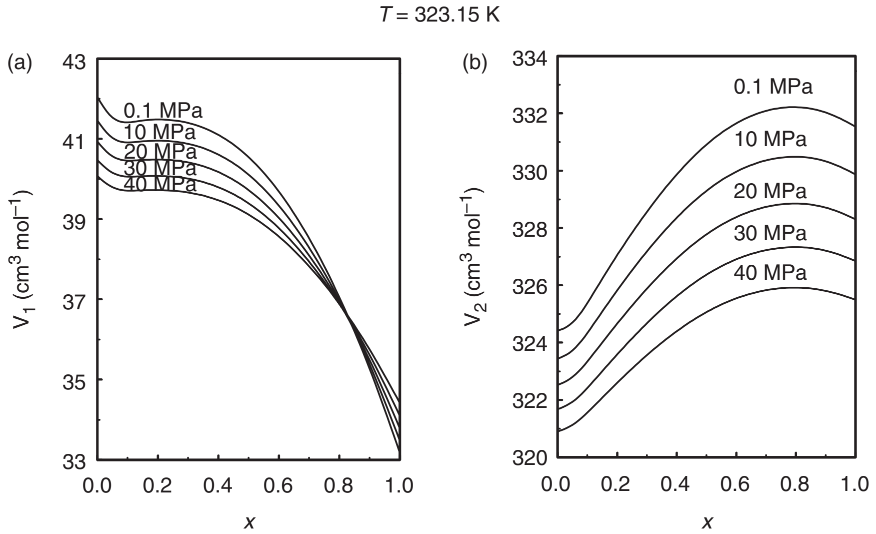

Figure 11. Partial molar volumes $\bar{V}_i$ $(i = 1, 2)$ as a function of concentration for selected isobars and at the selected temperature of 323.15 K.

(about 0.1 mole fraction of IL, for dilute mixture), while $\overline{V}_2 - x$ isotherm–isobar passes through a noticeable maximum at concentrations between 0.8 and −0.9 mole fraction of IL. These anomalies in the partial molar volumes at concentrations close to the pure component values (0 and 1 mole fraction) are more noticeable, manifesting at low pressures for the fixed temperature. The same anomalies in the partial molar volumes at low concentrations were also found previously for water + alcohol [42] and for methanol + $BMIMBF_4$ mixture (Abdulagatov *et al.* [15]). This is due to the rapid changing of the derivative $(\partial V_m/\partial x)_{pT}$ at the concentrations close to one of the pure components (near $x = 1.0$ or $x = 0.0$). The anomalous behaviour of the volumetric properties would be attributed to complex interaction between the hydrogen-bonded alcohol molecules and the IL anions.

The thermodynamic properties of infinite dilution mixtures can be calculated using the concept of the Krichevskii function [43–48], $J = (\partial p/\partial x)^{\infty}_{TV}$. The Tait EOS (6) was used to calculate the Krichevskii function for methanol + $[BMIM^+][OcSO_4^-]$ mixtures. The calculated values of the Krichevskii function for this mixture as a function of density for the selected isotherms are shown in Figure 12. As Figure 12 shows, the Krichevskii function for methanol + $[BMIM^+][OcSO_4^-]$ mixtures is negative and monotonically increasing (absolute values) with density. The negative values of the Krichevskii function mean that the interaction between the methanol molecules and IL ions is attractive. The Krichevskii function has a simple physical meaning, namely, it reflects the variation of the pressure of the system when exchanging a solvent (methanol) molecule by one solute molecule or ions (ILs) at constant volume and temperature. The values of $J$ connect straightforwardly to the direct (DCFI) and total (TCFI) correlation function integrals (see below) [43–54], i.e. they directly take into account the effects of the intermolecular interactions between neutral molecules of solvent (methanol) and solute (ILs) ions that determine the thermodynamic and structural properties of dilute mixtures. In general, the thermodynamic behaviour of infinitely dilute mixtures can be completely characterised by the Krichevskii function which is equal to the derivative $(\partial p/\partial x)_{TVx=0}$ calculated at fixed

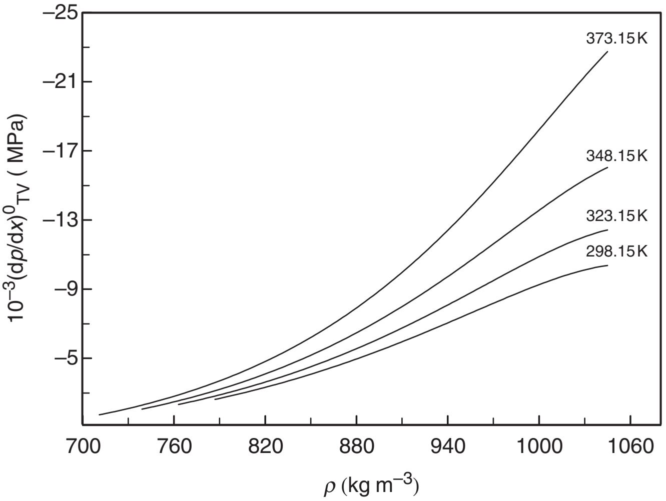

Figure 12. Density dependence of the Krichevskii function for various selected temperatures calculated with the Tait EOS (6).

temperature and volume as $x \to 0$. The Krichevskii function changes slightly with temperature at low densities, while at higher densities the changes are very essential.

The correlation function integrals technique is a very useful method with which to study the structural and thermodynamic properties of dilute mixtures. Kirkwood and Buff [55] (see also [56,57]) showed that thermodynamic properties of fluid mixtures can be expressed in terms of DCFI and TCFI. It is well known that the thermodynamic behaviour of dilute mixtures depends on microscopic phenomena involving local density perturbations induced by the presence of the solute molecules. Therefore, the thermodynamic behaviour of dilute mixtures is extremely important for the understanding of solute and solvent molecular interactions and the microscopic structure of solutions. The Krichevskii function is related to the TCFI [58]:

$$\left(\frac{\partial p}{\partial x}\right)^{\infty}_{TV} = \frac{\rho(H_{11} - H_{12})}{K_T}, \tag{13}$$

where $H_{11}$ and $H_{12}$ are the TCFI defined as $H_{ij} = \int h_{ij}(r)\mathrm{d}r$; $h_{ij}(r) = g_{ij}(r) - 1$ is the total correlation function for $i$–$j$ pair interactions; $g_{ij}(r)$ is the radial distribution function; $H_{11} = (K_T RT) - \rho^{-1}$ is the TCFI for $i$–$i$ pair (pure solvent molecules) interactions; and $K_T$ and $\rho$ are the isothermal compressibility and density of pure solvent (methanol), respectively. In terms of the direct correlation function, $c_{ij}(r)$, for $i$–$j$ pair interactions, the Krichevskii function $J$ is defined as [51,58–60]:

$$J = RT\rho^2(C_{11} - C_{12}), \tag{14}$$

where $C_{11}$ and $C_{12}$ are the DCFIs defined as $C_{ij} = \int c_{ij}(r)\mathrm{d}r$, and $(1 - \rho C_{11}) = (\rho K_T RT)^{-1}$ is the DCFI for $i$–$i$ (pure solvent molecules) pair interactions. The DCFI are related to the TCFI by the integrated Ornstein–Zernike equation [58], as:

$$H_{12} = C_{12} + \rho C_{12} H_{11}. \tag{15}$$

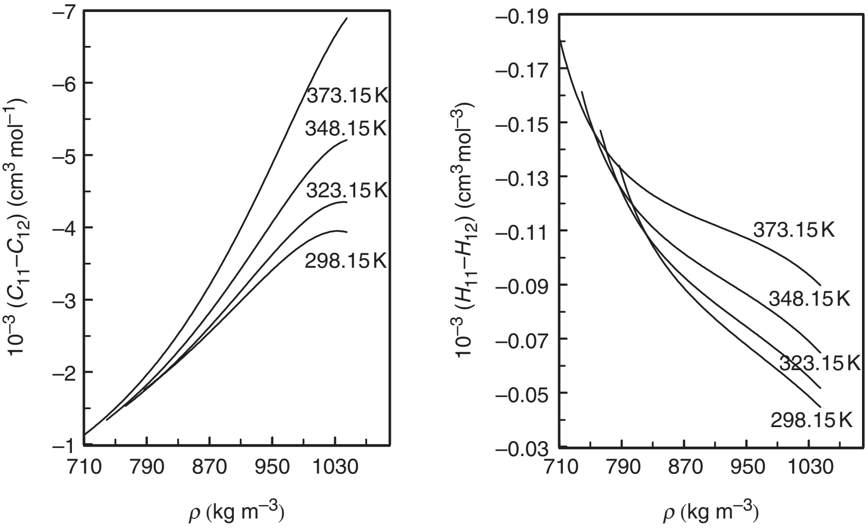

Figure 13. Direct ($C_{11}$–$C_{12}$) and total ($H_{11}$–$H_{12}$) correlation function integral differences for 1–1 and 1–2 pair interactions between methanol–methanol molecules and methanol–[BMIM$^+$][OcSO$_4^-$] (ions) as a function of density for various selected isotherms.

The differences between direct ($C_{11}$–$C_{12}$) and total ($H_{11}$–$H_{12}$) correlation function integrals of solute–solvent ([BMIM$^+$][OcSO$_4^-$] and methanol) and solvent–solvent (methanol–methanol) molecules as a function of the pure solvent (methanol) density calculated with Equations (13) and (14) using the Krichevskii function are presented in Figure 13 for various selected isotherms. The comparison between $C_{11}$ and $C_{12}$ and $H_{11}$ and $H_{12}$ for a selected isotherm of 323.15 K is also shown in Figure 14.

The DCFI ($C_{12}$) and TCFI ($H_{12}$) can also be expressed by partial molar volume at infinity dilution as

$$-C_{12} = \frac{\bar{V}_2^0}{K_T RT\rho} - V \quad \text{and} \quad \bar{V}_2^0 = V + (H_{11} - H_{12}). \tag{16}$$

Equation (16) can be used to calculate the DCFI and TCFI from the derived values of $V_\phi^0$ or $\bar{V}_2^0$, therefore, to calculate the microscopic intermolecular potential function parameters using the relation between the direct and total correlation functions and interaction potential function $u_{ij}(r)$ (Percus–Yevick approximation). The values of the Krichevskii function, $(\partial p/\partial x)_{TV}^{\infty}$, also associated with the behaviour of the microstructure of the dilute mixture (see below, Equation 17), measures the finite microscopic rearrangement of the solvent structure (methanol) around the infinitely dilute solute (ILs) relative to the solvent structure of ideal solution. The radial distribution function $g_{ij}(r)$ suggests that the individual molecules in methanol or ions in ILs tend to aggregate into molecule or ion clusters. The Krichevskii function defines the structural properties of infinite dilute mixtures, namely, the excess number of solvent (methanol) molecules $N_{exc}^{\infty}$ (structural parameter) around the infinitely dilute solute ([BMIM$^+$][OcSO$_4^-$]) relative to that number around any other solvent (methanol) molecule as [59,60]

$$N_{exc}^{\infty} = -K_T \left(\frac{\partial p}{\partial x}\right)_{TV}^{\infty}, \tag{17}$$

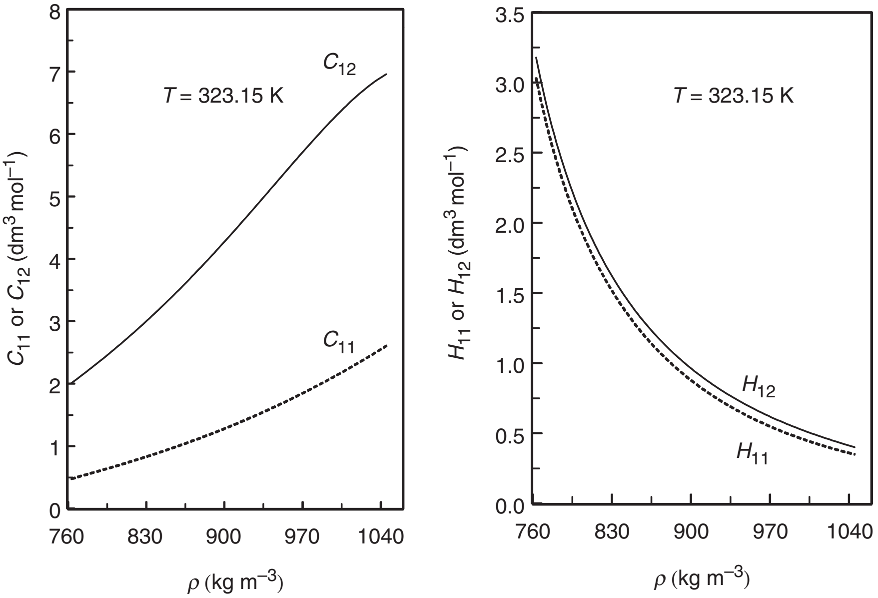

Figure 14. Direct ($C_{ij}$) and total ($H_{ij}$) correlation function integrals for 1–1 and 1–2 pair interactions between methanol–methanol and methanol–IL ions as a function of density for a selected isotherm of 323.15 K.

where

$$N^{\infty}_{exc} = 4\pi\rho \int_0^{R_{shell}} [g_{12}(r) - g_{11}(r)]r^2 \mathrm{d}r \tag{18}$$

is the definition of the excess number of solvent (methanol) molecules surrounding IL ions. As one can see from (17), $N^{\infty}_{\mathrm{exc}} + N_{12} - N_{11}$, where $N_{12} = 4\pi\rho \int_0^{R_{shell}} g_{12}(r)r^2 \mathrm{d}r$ and $N_{11} = 4\pi\rho \int_0^{R_{shell}} g_{11}(r)r^2 \mathrm{d}r$ are the coordination numbers for the first solvation shell (molecule clusters). $N_{12}$ indicates the number IL ions surrounded by a cage of $N_{12}$ molecules of methanol, while $N_{11}$ indicates that each methanol molecule in the bulk is surrounded by a cage of $N_{11}$ other methanol molecules. Figure 15 shows the density dependence of the excess number of solvent (methanol) molecules, $N^{\infty}_{\mathrm{exc}}$, around the infinitely dilute solute ([BMIM$^+$][OcSO$_4^-$]) along the various isotherms calculated from Equation (17) using the isothermal compressibility of pure methanol (IUPAC EOS [19]) and derived (from the present density measurements) values of the Krichevskii function. As one can see from Figure 15, the excess number of solvent (methanol) molecules $N^{\infty}_{\mathrm{exc}}$ around the IL ions in the infinite dilution limit is positive (the Krichebskii parameter is negative, $(\partial p/\partial x)^{\infty}_{TV} < 0$). This means that $N_{12} > N_{11}$, or, in other words, when exchanging a solvent (methanol) molecule by one solute (IL) ions at constant volume and temperature, the local density of methanol molecules around IL ions increases from 2 to 5 depending on $T$ and $p$ compared with the ideal mixture or bulk density of pure methanol (local environment around an infinitely dilute IL differs from the bulk average). Thus, methanol + [BMIM$^+$][OcSO$_4^-$] is an 'attractive' mixture, $(\partial p/\partial x)^{\infty}_{TV} < 0$ [45,48], $N^{\infty}_{\mathrm{exc}} > 0$, positive. Usually, coordination number $N_{ij}$ is calculated using MD or MK simulation

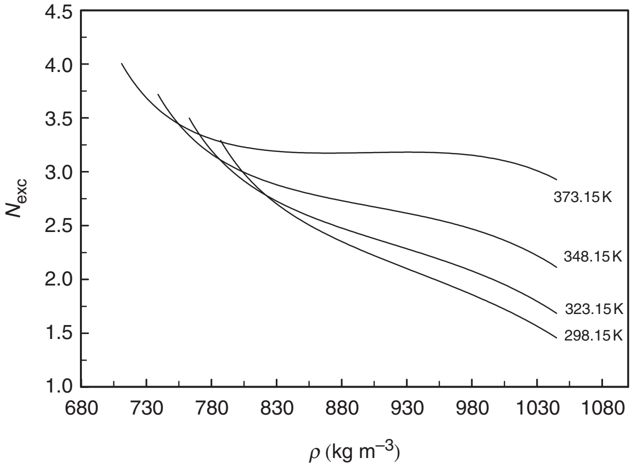

Figure 15. Number of methanol molecules (cluster size or excess coordination number, $N_{exc}$) around IL ions in excess of that found around a methanol molecule, as a function of density along various isotherms.

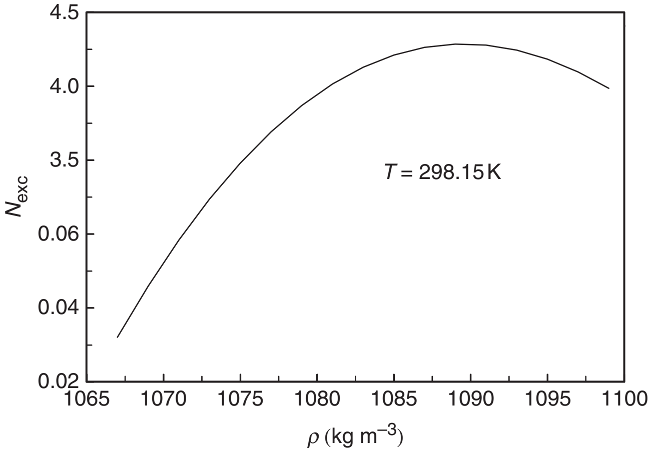

Figure 16. Number of IL ions around a methanol molecule in excess of that found around an IL ion, as a function of density along selected isotherm and at 0.1 MPa.

studies with various radial distribution functions, see, for example, [61,62]. For example, Morrow and Maginn [61] found for ILs ([BMIM$^+$][$PF_6^-$]) that total coordination number for the first solvation shell of an ion is nearly 13 at 298 K and 0.98 bar. Liu *et al.* [62] also found that the coordination number for ILs ([EMIM$^+$][$BF_4^-$], [BMIM$^+$][$BF_4^-$], [BMIM$^+$][$PF_6^-$], [DMIM$^+$][$PF_6^-$], and [DMIM$^+$][$Cl^-$]) from MD studies (calculated from radial distribution function by integrating from zero to the first minimum, $R_{\text{shell}}$) are within 6–7 counter-ions surrounding each ion at 298 K and 1 bar. The excess number of IL ([BMIM$^+$][OcSO$_4^-$]) ions $N_{\text{exc}}^{\infty}$ around the infinitely dilute solute (methanol) relative to the number around any other IL ions using the relation (17) for $x \rightarrow 1$ (dilute mixture when IL is solvent, methanol is solute) at 298.15 K and at pressures from 0.1 to 50 MPa (Figure 16) was also calculated. Because of the Krichevskii function $(\partial p/\partial x)_{TV}^{\infty}$ for dilute mixtures,

$[BMIM^+][OcSO_4^-]$ + methanol ($x \to 1$) is relatively small, and the values of excess coordination number $N_{exc}^{\infty}$ are also very small (almost zero). Microscopically, it means that when exchanging solvent ($[BMIM^+][OcSO_4^-]$) ions by one solute (methanol) molecule at constant volume and temperature, the local density of IL ions around the methanol molecule is nearly not changing, compared with the ideal mixture or bulk density of pure ILs i.e. the local environment (microstructure) around an infinitely dilute solute (methanol) does not change. Therefore, if we assume that the coordination number in ILs [62] is about $N_{11} = 6$–7, the coordination number for $N_{12} = N_{exc}^{\infty} + N_{11}$ is the same (within 6–7), because $N_{exc}^{\infty} \approx 0$, $N_{12} = N_{exc}^{\infty}$.

## 4. Conclusions

Density measurements ($p, \rho, T$ data) and derived properties such as excess, partial and apparent molar volumes $V_\phi$ of $[BMIM^+][OcSO_4^-]$ in methanol at $T = (298.15$–$398.15\,K)$, pressures up to $p = 40\,MPa$ for six compositions $x = (0.0388, 0.1351, 0.2785, 0.4961, 0.7497, 0.9312$ and pure $[BMIM^+][OcSO_4^-]$) mole fraction of $[BMIM^+][OcSO_4^-]$ are reported. Measured densities were used to develop accurate Tait-type EOS for the pure component and the mixture. This EOS represents the present density data within 0.05% (for methanol), 0.016% (for ILs) and 0.19% (for mixture). The excess molar volume for this mixture is negative at any measured temperatures, pressures and concentrations with observed concentration minimum between 0.2 and 0.3 mole fraction of ILs. The derived apparent molar volumes, $V_\phi$, were used to calculate the apparent molar volumes (or partial molar volumes) at infinite dilution, $V_\phi^0$, using Pitzer's ion-interaction model. Derived values of $V_\phi$ at low concentration (for dilute mixtures) and $V_\phi^0$ exhibit the maximum at temperatures around 350 K, while at high concentrations they are almost a linear function of temperature. The method of correlation integrals is applied to study the structural and thermodynamic properties of dilute methanol + $[BMIM^+][OcSO_4^-]$ mixtures. DCFI and TCFI for 1–1 (methanol–methanol) and 1–2 (methanol–ILs) pair interactions, and the excess number of solvent (methanol) molecules $N_{exc}^{\infty}$ around ILs ions was calculated using the Krichevskii function. It was found that the excess coordination number of solvent (methanol) molecules, $N_{exc}^{\infty}$, around the infinitely dilute solute ($[BMIM^+][OcSO_4^-]$) at temperatures from 298 to 373 K and at pressures up to 40 MPa varies within 2–5.

## Acknowledgements

I.M. Abdulagatov thanks the Physical and Chemical Properties Division at the National Institute of Standards and Technology for the opportunity to work as a Guest Researcher at NIST during the course of this research. J.T. Safarov thanks the Alexander von Humboldt Foundation for his research period at the University of Rostock, Germany.

## References

[1] R.F. de Souza, J.C. Padilha, R.S. Goncalves, and J. Dupont, Electrochem. Commun. **5**, 728 (2003).
[2] C.C. Tzschuncke, C. Markert, W. Bannwarth, S. Roller, A. Hebel, and R. Haag, Angew. Chem. Int. Ed. **41**, 3964 (2002).
[3] L.A. Blanchard, D. Hancu, E.J. Beckman, and J.F. Brennecke, Nature **399**, 28 (1999).

[4] R.A. Sheldon, R.M. Lau, M.L. Sorgedrager, F. vaan Rantwijk, and K.R. Sedon, Green Chem. **4**, 147 (2002).
[5] J.F. Brennecke and E.J. Maginn, AIChE J. **47**, 2384 (2001).
[6] S.G. Cull, J.D. Holbrey, V. Vargas-Mora, K.R. Seddon, and G.J. Lye, Biothechnol. Bioeng. **69**, 227 (2000).
[7] H. Zhao, J. Phys. Chem. Liq. **41**, 545 (2003).
[8] J.D. Holbrey and K.R. Seddon, J. Chem. Soc., Dalton Trans. **13**, 2133 (1999).
[9] U. Domańska, A. Pobudkowska, and A. Wiśniewska, J. Sol. Chem. **35**, 311 (2006).
[10] H. Machida, Y. Sato, and R.L. Smith Jr, Fluid Phase Equilib. **264**, 147 (2008).
[11] M.J. Dávila, S. Aparicio, R. Alcalde, B. Garcia, and M.J. Leal, Green Chem. **9**, 221 (2007).
[12] A. Wandschneider, A. Lehmann, and A. Heintz, J. Chem. Eng. Data **53**, 596 (2008).
[13] I.M. Abdulagatov, A. Tekin, J. Safarov, A. Shahverdiyev, and E. Hassel, Int. J. Thermophys. **29**, 505 (2008).
[14] I.M. Abdulagatov, A. Tekin, J. Safarov, A. Shahverdiyev, and E. Hassel, J. Sol. Chem. **37**, 801 (2008).
[15] I.M. Abdulagatov, A. Tekin, J. Safarov, A. Shahverdiyev, and E. Hassel, J. Chem. Thermodyn. **40**, 1386 (2008).
[16] I.M. Abdulagatov, J. Safarov, F. Aliyev, M. Talibov, A. Shahverdiyev, and E. Hassel, Fluid Phase Equilib. **268**, 21 (2008).
[17] I.M. Abdulagatov, J. Safarov, T. Guliyev, A. Shahverdiyev, and E. Hassel, J. Chem. Eng. Data **268**, 21 (2008).
[18] W. Wagner and A. Pruß, J. Phys. Chem. Ref. Data **31**, 387 (2002).
[19] K.M. de Reuck and R.J.B. Craven, *Methanol. International Thermodynamic Tables of the Fluid State-12* (Blackwell Scientific, Oxford, 1993).
[20] E.C. Ihmels, J. Safarov, E. Hassel, and J. Gmehling, J. Chem. Thermodyn. **37**, 1318 (2005).
[21] J. Wang, Y. Tian, Y. Zhao, and K. Zhao, Green Chem. **5**, 618 (2003).
[22] I.M. Abdulagatov and N.D. Azizov, J. Thermal Analysis Calorim. **87**, 483 (2007).
[23] I.M. Abdulagatov and N.D. Azizov, J. Chem. Thermodyn. **38**, 1402 (2006).
[24] E.J. González, L. Alonso, and À. Domínguez, J. Chem. Eng. Data **51**, 1446 (2006).
[25] Z. Atik, J. Chem. Thermodyn. **38**, 201 (2006).
[26] B. Orge, M. Iglesias, A. Rodrígues, J. Canosa, and J. Tojo, Fluid Phase Equilib. **133**, 213 (1997).
[27] W.J. Magee and I.M. Abdulagatov, Fluid Phase Equilib. **217**, 45 (2004).
[28] A. Rodrígez, J. Canosa, and J. Tojo, J. Chem. Thermodyn. **33**, 1383 (2001).
[29] K.S. Pitzer, J. Phys. Chem. **77**, 268 (1973).
[30] D.J. Bradley and K.S Pitzer, J. Phys. Chem. **83**, 1599 (1979).
[31] I.M. Abdulagatov, N.D. Azizov, and A.B. Zeinalova, Phys. Chem. Liquids **45**, 127 (2007).
[32] I.M. Abdulagatov and N.D. Azizov, J. Sol. Chem. **32**, 573 (2003).
[33] Z. Gu and J.F. Brennecke, J. Chem. Eng. Data **47**, 339 (2002).
[34] E.C. Ihmels and J. Gmehling, Ind. Eng. Chem. Res. **40**, 4470 (2001).
[35] R.L. Gardas, M.G. Freire, P.J. Carvalho, I.M. Marrucho, I.M.A. Fonseca, A.G.M. Ferreira, and J.A.P.J. Coutinho, J. Chem. Eng. Data **52**, 80 (2007).
[36] M.J. Assael, J.H. Dymond, and D. Exadaktilou, Int. J. Thermophys. **15**, 155 (1994).
[37] J.H. Dymond and R. Malhotra, Int. J. Thermophys. **9**, 941 (1988).
[38] J.H. Dymond, R. Malhotra, J.D. Isdale, and N.F. Glen, J. Chem. Thermodyn. **20**, 603 (1988).
[39] A. Kumagai, K. Date, and H. Iwasaki, J. Chem. Eng. Data **21**, 226 (1976).
[40] H.J. Albert, J.A. Gates, R.H. Wood, and J.-P.E. Grolier, Fluid Phase Equilib. **20**, 321 (1985).
[41] T. Hofman, A. Goldon, A. Nevines, and T.M. Letcher, J. Chem. Thermodyn. **40**, 580 (2008).
[42] H. Kubota, Y. Tanaka, and T. Makita, Int. J. Thermophys. **8**, 47 (1987).
[43] Y. Hiejima and M. Yao, J. Chem. Phys. **119**, 7931 (2003).
[44] J.M.H. Levelt Sengers, G. Morrison, G. Nielson, R.F. Chang, and C.M. Everhart, Int. J. Thermophys. **7**, 231 (1986).
[45] J.M.H. Levelt Sengers, J. Supercrit. Fluids **4**, 215 (1991).

[46] R.F. Chang and J.M.H. Levelt Sengers, J. Phys. Chem. **90**, 5921 (1986).
[47] A.A. Chialvo and P.T. Cummings, AIChE J. **40**, 1558 (1994).
[48] P.G. Debenedetti and R.S. Mohamed, J. Chem. Phys. **90**, 4528 (1989).
[49] R.F. Chang, G. Morrison, and J.M.H. Levelt Sengers, J. Phys. Chem. **88**, 3389 (1984).
[50] A.H. Harvey and J.M.H. Levelt Sengers, J. Phys. Chem. **95**, 932 (1991).
[51] R. Fernández-Prini and M.L. Japas, Chem. Soc. Rev. **23**, 155 (1994).
[52] J.P. O'Connell, Y. Hu, and K.A. Marshall, Fluid Phase Equilib. **158**, 583 (1999).
[53] H.D. Cochran, L.L. Lee, and D.M. Pfund, in *Fluctuation Theory of Mixtures*, edited by E. Matteoli and G.A. Manssori (Taylor and Francis, New York, 1990), pp. 69–93.
[54] A.A. Chialvo and P.T. Cummings, AIChE J. **44**, 667 (1998).
[55] J.G. Kirkwood and F.P. Buff, J. Chem. Phys. **19**, 774 (1951).
[56] A. Ben-Naim, *Water and Aqueous Solutions* (Plenum, New York, 1974).
[57] A. Munster, in *Fluctuation Phenomena in Solids*, edited by R.E. Burgess (Academic Press, New York, 1965).
[58] D.B. McGuigan and P.A. Monson, Fluid Phase Equilib. **57**, 227 (1990).
[59] S.W. Brelvi and J.P. O'Connell, AIChE J. **18**, 1239 (1972).
[60] J.P. O'Connell, Mol. Phys. **20**, 27 (1971).
[61] T.I. Morrow and E.J. Maginn, J. Phys. Chem. B. **106**, 12807 (2002).
[62] Z. Liu, Sh. Huang, and W. Wang, J. Phys. Chem. B. **108**, 12978 (2004).